

AD-A198 477

DTIC FILE COPY

④

TECHNICAL REPORT NO. 10

TO

The Office of Naval Research
Contract no. NOOO14-86-K-0381

THE INFLUENCE OF POROSITY ON SHORT FATIGUE CRACK GROWTH
AT LARGE STRAIN AMPLITUDES

D. A. Gerard and D. A. Koss

Department of Materials Science and Engineering
The Pennsylvania State University
University Park, PA 16802

Reproduction In Whole Or In Part Is Permitted
For Any Purpose Of The United States Government
Distribution Of This Document Is Unlimited

DTIC
ELECTE
AUG 26 1988
S H D

88 8 25 188

REPORT DOCUMENTATION PAGE		READ INSTRUCTIONS BEFORE COMPLETING FORM
1. REPORT NUMBER Technical Report No. 10	2. GOVT ACCESSION NO.	3. RECIPIENT'S CATALOG NUMBER
4. TITLE (and Subtitle) The Influence of Porosity on Short Fatigue Crack Growth at Large Strain Amplitudes.		5. TYPE OF REPORT & PERIOD COVERED
		6. PERFORMING ORG. REPORT NUMBER
7. AUTHOR(s) D. A. Gerard D. A. Koss		8. CONTRACT OR GRANT NUMBER(s) N00014-86-K-0381
9. PERFORMING ORGANIZATION NAME AND ADDRESS Department of Materials Science and Engineering The Pennsylvania State University University Park, PA 16802		10. PROGRAM ELEMENT, PROJECT, TASK AREA & WORK UNIT NUMBERS
11. CONTROLLING OFFICE NAME AND ADDRESS Office of Naval Research 800 N. Quincy St. Arlington, VA 22217		12. REPORT DATE July 1988
		13. NUMBER OF PAGES
14. MONITORING AGENCY NAME & ADDRESS (if different from Controlling Office)		15. SECURITY CLASS. (of this report)
		15a. DECLASSIFICATION/DOWNGRADING SCHEDULE
16. DISTRIBUTION STATEMENT (of this Report) Distribution of this document is unlimited.		
17. DISTRIBUTION STATEMENT (of the abstract entered in Block 20, if different from Report)		
18. SUPPLEMENTARY NOTES		
19. KEY WORDS (Continue on reverse side if necessary and identify by block number) Short crack growth, porosity, low cycle fatigue, titanium. (JES)		
20. ABSTRACT (Continue on reverse side if necessary and identify by block number) The influence of the pore microstructure (0% to 6% rounded porosity isolated vs. interconnected) on short crack growth behavior during low cycle fatigue has been evaluated using powder-processed titanium as a model system. The presence of porosity enhances short crack propagation adjacent to the pores as a result of localized, pore-induced plasticity. Observations of short cracks using surface replicas indicate that once a crack extends beyond a plastic zone of an isolated pore it decelerates to propagation rates similar to those observed for fully dense materials of the similar grain sizes. For		

Block #20

low levels of porosity in which the pores are isolated, the vast majority of short crack growth occurs outside the regions of highly localized strain, and thus the overall short crack growth are not significantly affected. However, when the pores are interconnected the short cracks are consistently observed to propagate at higher rates of growth than cracks of comparable size in the fully dense material. The enhanced growth rates appear to be a result of the continuous nature of the plastic zones which provide a high strain amplitude propagation path.

Accession For	
NTIS GRA&I	<input checked="" type="checkbox"/>
DTIC TAB	<input type="checkbox"/>
Unannounced	<input type="checkbox"/>
Justification	
By	
Distribution/	
Availability Codes	
Avail and/or	
Dist	Special
A-1	

THE INFLUENCE OF POROSITY ON SHORT FATIGUE CRACK GROWTH AT LARGE STRAIN AMPLITUDES

D. A. Gerard and D. A. Koss

The Department of Materials Science and Engineering

The Pennsylvania State University

University Park, PA 16802

Abstract:

The influence of the pore microstructure (0% to 6% rounded porosity isolated vs. interconnected) on short crack growth behavior during low cycle fatigue has been evaluated using powder-processed titanium as a model system. The presence of porosity enhances short crack propagation adjacent to the pores as a result of localized, pore-induced plasticity. Observations of short cracks using surface replicas indicate that once a crack extends beyond a plastic zone of an isolated pore it decelerates to propagation rates similar to those observed for fully dense materials of the similar grain sizes. For low levels of porosity in which the pores are isolated, the vast majority of short crack growth occurs outside the regions of highly localized strain, and thus the overall short crack growth rates are not significantly affected. However, when the pores are interconnected the short cracks are consistently observed to propagate at higher rates of growth than cracks of comparable size in the fully dense material. The enhanced growth rates appear to be a result of the continuous nature of the plastic zones which provide a high strain amplitude propagation path.

Introduction:

It is well documented that during the fatigue testing of fully dense materials short cracks frequently propagate at higher rates of growth than larger cracks subjected to the same nominal driving force.^(1,2) Despite many studies of short crack growth in fully dense metals, there has been no previous investigation which has examined the influence of porosity on short fatigue crack growth behavior. This is the case even though the pores initiate numerous short cracks and therefore the potential for large accelerations in crack growth behavior exist in metals containing porosity. It is significant that several studies have observed large accelerations in short fatigue crack growth rates adjacent to isolated macroscopic notches (~ 1 mm radius) as well as microscopic notches (≤ 100 μ m radius) under conditions of small strain amplitudes.⁽³⁻⁸⁾ The enhanced propagation rates have been attributed to accelerated damage resulting from a region of plastic strains which develops adjacent to a defect in a nominally elastically deforming matrix.

In view of the observations for crack growth and isolated notches, the potential for a sustained enhancement short fatigue crack growth rates exists when defects such as pores are present. In particular, at a given stress or strain amplitude, a sustained enhancement in the short fatigue crack growth rates may occur when the plastic zones adjacent to the pores are large and/or overlap, such as during low cycle fatigue wherein the entire matrix is fully plastic. Thus, the purpose of this study is to determine to what extent pores act to influence short crack growth in the fully plastic low cycle fatigue regime. Specifically, the objective of this investigation is to examine the influence of porosity (0% to 6% rounded porosity, discontinuous vs. continuous) on naturally forming short fatigue cracks propagating in a plastically deforming powder-processed titanium matrix. Results from this investigation should be pertinent to short

fatigue crack growth during low cycle fatigue for a broad range of materials which either (a) inherently have pores, such as powder-processed or cast materials, or (b) readily initiate voids at small plastic strains such as at a weak matrix/inclusion interface.

Material Characterization and Experimental Procedure:

Conventional powder metallurgy processing techniques using the sequential processes of cold isostatic pressing, sintering, swaging, and resintering were used to prepare low cycle fatigue specimens of commercially pure titanium which was used as a model material for this study. See Table I for the processing histories. Wrought titanium having essentially the same impurity content as the powder-processed specimens was used for comparing the short crack growth properties of the fully dense and porous conditions; see Table II. The fully dense and porous microstructures containing 1.5% and 6% isolated porosity as well as 6% interconnected porosity are shown in Fig. 1. Stereopycnometer results confirmed that the pores were isolated in two of the porous conditions (Fig. 1b and 1c) and completely interconnected in the other condition examined (Fig. 1d). The microstructures in the isolated porosity specimens consist of well rounded elliptical pores having average radius* of 10 to 15 microns and an average aspect ratio (major/minor diameter) of 1.3. Fig. 1d shows that when the interconnected porosity (of the second group of 6% porous specimens) is examined in cross section the pores are well rounded and generally appear to be nearly elliptical in shape. These pores have an average radius of about 25 microns, and an average aspect ratio of 1.9. It

* The average radius is the average value of the Martin radii. In this study, the Martin radii are defined as the distance from the center of gravity of the pore to its edge; the initial radius measurement is taken at an arbitrary angle of 0° after which the remaining radii are obtained at angles of 45°, 90°, 135°, 180°, 225°, 270°, and 315°.

should also be noted that for each of the conditions the grain size was of the same order of magnitude in size as the pores, ranging from a 40 μm diameter in the fully dense and 6% isolated porous materials to 100 μm in the 1.5% porous condition (Table I).

Fully reversible low cycle fatigue tests were performed at room temperature in total strain control at amplitudes of .75 and 1.5%. The lower strain amplitude tests were conducted at a frequency of .25 Hz while the larger amplitude tests have been performed at .15 Hz, both with a triangular waveform. Cylindrical push-pull low cycle fatigue specimens were used in this study; the specimens had a gage length of 15 mm and a 6.4 mm diameter.

In order to monitor short fatigue crack growth rates, the low cycle fatigue tests were periodically interrupted and acetate surface replicas were taken. During each interruption the entire gage section of the specimen was examined using a replicating technique which was developed utilizing a surface replicating application tool. The tool consists of a cylindrical shell of brass with an inner layer of polymeric material (Tygon™) whose inner radius equals that of the gage section of the specimen. The combination of the flexible polymer and the rigid brass distributed loads to the replicating tape uniformly over a relatively large area while allowing the acetate tape to flow against the surface features. After application, the replicas were flattened using a procedure described elsewhere.⁽⁹⁾

In order to estimate short crack propagation rates, the cyclic J-integral range ΔJ was utilized.⁽¹⁰⁻¹²⁾ To calculate ΔJ , the measured surface crack length must be converted to a crack depth. A standard heat tinting technique which is described elsewhere⁽⁹⁾ was used to estimate the short crack crack-front shapes. Measurements of the ratio of the depth to surface length indicated that the short crack cracks have a ratio of approximately 0.4 for each of the porous conditions

being of a thumb-nail type shape with irregularities on the order of the pore sizes; this ratio is in agreement with the crack shapes observed in fully dense materials in other investigations^(13,14). The short crack shapes were evaluated over a distribution of crack sizes ranging from 40 to 1300 μ m in surface length. In addition to measuring crack growth rates, crack closure was also monitored by periodically stopping tests and making surface replicas at varying loads throughout a single hysteresis loop. Crack closure loads could then be determined by examining gold coated surface replicas in a scanning electron microscope. A crack closure load could be estimated by observing microstructural features on both sides of a crack as a function of the load. Once crack closure occurs, the microstructural features should appear to remain a constant distance apart (at least within the resolution of this measuring technique) during increasing compressive loads.

Experimental Results:

Fig. 2 illustrates the influence of isolated porosity on the growth of fatigue cracks during fully reversed plastic cycling. These data present the crack growth rates da/dN in terms of the cyclic crack growth resistance ΔJ . In this study, ΔJ is calculated for fully plastic crack growth using the formulation developed by Dowling⁽¹⁰⁻¹²⁾ for estimating short and long crack growth rates at large strain amplitudes in steels. The basis for Dowling's ΔJ analysis has been discussed in detail elsewhere,⁽¹²⁾ and it should be noted that Dowling's work has been experimentally verified in several other investigations.⁽¹⁴⁻¹⁹⁾ The magnitude of ΔJ can be calculated utilizing the following expression:

$$\Delta J = a^* \beta^* (\Delta W_e + f(n') * \Delta W_p), \quad (1)$$

where a is the crack depth, β is a crack-shape constant, $f(n')$ is a boundary condition which is a function of the cyclic work hardening exponent n' , and ΔW_e and ΔW_p are global elastic and plastic energies which are obtained from stress-strain hysteresis loops. In order to measure the actual driving force for the growth of short cracks an effective cyclic ΔJ_{eff} , which is analogous to ΔK_{eff} , is obtained by measuring crack closures.⁽¹⁹⁾ As is the case for ΔK_{eff} , ΔJ_{eff} is calculated from the portion of the hysteresis cycle where the crack-tip is open. The evaluation of gold coated acetate surface replicas on a scanning electron microscope indicate that in the present study the short cracks remained open to at least within 3% of the maximum compressive stress; these results agree with Wagner and Lütjering⁽²⁰⁾ who observed that short cracks in an ($\alpha + \beta$) titanium alloy remained open during the entire compressive loading portion of the hysteresis cycling. Thus in this study we assume that $\Delta J_{eff} \approx \Delta J$.

The two solid lines in each part of Fig. 2 indicate a range of data and are based on an extrapolation of the fatigue crack growth rates da/dN as a function of the stress intensity range ΔK for the growth of large cracks in fully dense titanium as measured by under linear elastic fracture mechanic conditions.⁽²¹⁾ These data have been obtained from titanium of similar impurity content to that used in this investigation. In addition, the long crack data have been determined at a high R ratio ($\sigma_{max}/\sigma_{min} = 0.7$), and thus the crack closure should not have a significant effect on the large crack propagation rates.

The short crack growth data shown in each section of Fig. 2 corresponds to growth rates obtained from multiple cracks. In order to interpret these data correctly, it must also be recognized that the cyclic J-integral is proportional to the crack depth ($\Delta J \propto a$). Thus, in comparing the crack growth rates from each of the different material conditions, the propagation rates should be examined at approximately the same ΔJ and thus the same a . Thus, Fig. 2 demonstrates that

at total strain amplitude testing of 1.5%, short fatigue cracks in both the fully dense and the porous materials frequently propagate at higher rates of growth than large fatigue cracks under similar crack growth driving forces. However, in directly comparing Fig. 2a to the data in Fig. 2b thru 2c, it is also apparent that the short fatigue cracks within the fully dense and the materials containing isolated porosity are often growing at approximately the same rates, except for some temporary increases in the crack growth rates of the porous specimens. These comparisons are more apparent in Fig. 3 which combines the data of Fig. 2a and 2c in order to compare the crack growth rates for the fully dense and the 6% isolated porosity titanium. Fig. 3 clearly illustrates that there is a large range of crack growth rates in the porous material with some rates showing significant accelerations which others are similar in magnitude to those of short (and long) cracks in fully dense titanium.

Once the porosity becomes interconnected, results such as those in Fig. 2d and Fig. 4 indicate that there is a significant pore-induced acceleration of growth rates. The material containing interconnected porosity typically exhibits two to ten times higher values of da/dN at the same ΔJ -value.

Short crack growth rates for the fully dense and porous titanium were also obtained at a total strain amplitude of 0.75%. As shown in Fig. 5, the results are similar to those obtained at 1.5% total strain amplitude.

Examination of the surface replicas indicate that the temporary increases in short crack propagation rates generally occur when the propagating crack-tip is in the vicinity of a pore or another crack. Specifically, the enhancement in the short crack growth rates were observed to occur when a crack (a) initiated at a pore and had a crack length roughly less than the pore diameter, (b) propagated through a pore, or (c) linked-up with another favorably oriented crack.

Discussion:

Anomalously high short crack growth rates have most frequently been attributed to crack closure and microstructural effects. As was previously discussed, an examination of surface replicas of the short cracks taken at various loads of a single hysteresis loop indicate the absence of crack closure (at least to within 3% of the maximum compressive stress) in both the fully dense and porous specimens. This absence of crack closure is a consequence of the large strain amplitudes used in this study and is in agreement with results of Wagner and Lütjering⁽²⁰⁾ for short cracks in an (alpha-beta) titanium alloy as well as for short and long crack data for a nodular iron and a steel subjected to fully reversible large strain amplitude fatigue testing^(16,22). The highly compressive crack closure loads (ref. 22) appear to be a result of the large crack advances which occur during the tensile portion of each cycle and the concomitant large crack opening displacements which overwhelm plasticity-induced and reduce roughness-induced closure effects (these are typically very significant effects during low stress or strain amplitude (i.e. elastic) fatigue testing). In view of the above, it is not surprising that crack closure is not observed in small cracks for the fully dense or porous specimens during large strain deformation of titanium. Thus, we conclude that in the present study crack closure does not significantly effect the short crack growth behavior of either the fully dense or the porous materials. Therefore, an interpretation of the short crack growth behavior must be made on the basis of microstructural effects, notably porosity.

In the absence of porosity the enhancement of short crack growth rates shown in Figs. 2, 3, 5 may be due to effects of microstructural dissimilitude as discussed by Chan and Lankford⁽²³⁾. For a pure polycrystalline metal, these authors suggest that fatigue cracks typically initiate in a grain which is

preferentially oriented for fatigue crack propagation. If grains adjacent the crack are not favorably oriented for crack growth then it will slow down and possibly arrest when the crack-tip approaches a barrier such as a grain boundary. On the contrary, if the adjacent grains are favorably oriented for crack growth, the short crack will be able to propagate at high rates through these grains as well. As crack growth occurs, the crack front encounters an increasingly larger number of grains and the growth rate will begin to be reduced as some grains along the crack-front will be favorably oriented for fatigue crack growth while others will not. Thus, when the crack-front of a short crack becomes microstructurally large (for example ~20 grains) it will begin to propagate in a continuum type manner transcending (and in some cases decelerating) into the large crack growth regime. In the present study, cracks initiate at pores and grow in the absence of crack closure at the large strain amplitudes. As will be discussed later, the scale of the porosity with respect the microstructure can be a significant factor in short crack growth of porous materials. In addition, analogous to a favorably oriented grain which provides an easy path for short fatigue crack propagation, we suggest that a pore can also enhance growth rates on a local scale as a result of the strain dissimilitude which develops in the microstructure.

A major observation of the present study is that although the short crack growth rates are significantly enhanced by the presence of isolated pores, this acceleration in growth only encompasses a region on the order of the size of the pore after which the crack propagates at rates similar to that as if it were in a fully dense material, at least until it encounters another pore or crack. Thus the overall individual short crack growth rates are not significantly affected by the presence of isolated porosity (at least at pore volume fractions typically ≤ 0.06 wherein the pores can be isolated). As described previously, the temporary

increases in short crack propagation rates occur when a crack (a) initiates at a pore, (b) propagates through a pore, or (c) links with another favorably oriented crack. In each of the above cases the crack-front encounters a defect which has generated a plastic zone that contains plastic strain amplitudes which (on a local scale) can vastly exceed the nominal strain amplitude in the plastically deforming matrix.

As a basis for illustrating the effects of locally large plastic strain amplitudes, Fig. 6 shows a schematic of a plastic strain profile adjacent to an elliptical hole; the magnitude of the local strain amplitude $\Delta\epsilon$ is determined along the plane of maximum strain concentration (i.e. perpendicular to the fatigue axis)*. As a result of the intensification of local strain amplitudes near holes (or pores) a temporary acceleration of short crack growth rates occurs as the cracks propagate through the plastic zones adjacent to the pores. This effect is shown schematically in Fig. 7 which indicates an initially high but decreasing crack growth rate which is attributed to the strain gradient present in the plastic zone adjacent to the elliptical hole which has a plastic zone size roughly equal to the hole size, as is shown in Fig. 6. Several investigators⁽⁴⁻⁸⁾ have measured crack growth profiles similar to that in Fig. 7a wherein the cracks were propagating plastic zones adjacent to notches embedded in an elastically deforming matrix. A major difference between the crack growth behavior in the presence of porosity and that near macroscopic holes is the size of the plastic zones with reference to the scale of the microstructure, notably the grain size. Thus, unlike a crack which has propagated through the plastic zone near a large notch or hole, a crack propagating through the plastic zone of a pore usually remains microstructurally short. This occurs since in this study the

* Verification of a plastic strain profile similar to that shown in Fig. 6 has been made under plane stress conditions in monotonic tension.⁽²⁴⁾

pores, and thus their plastic zones (see Fig. 6) are similar in size to the grain size (as is frequently the case in powder-fabricated metals). Once the tip of a short crack propagates beyond the plastic zone of a pore, its propagation rate will be controlled by the plasticity within and orientations of the pertinent grains. In summary, the magnitude of a pore-induced acceleration in short crack growth rate should be dependent on (1) the pore size, which scales the plastic zone associated with the pore (see Fig. 6), (2) the shape of the pore which will influence the $\Delta\epsilon_{\text{local}}$ near the pore, (3) the imposed strain amplitude which also affects the size of and strain intensity in the plastic zone, and (4) the size and orientation of the grains adjacent to the pores within which the short cracks propagate. A similar rationale based on localized plastic zones accounts for the acceleration in crack propagation rates noted when a short crack approaches another pore or microcrack on favorably oriented planes.

The results from this study also suggest that if the porosity should become interconnected or so closely spaced that there is significant overlap of the pore-induced plastic zones then the short crack growth rates would be expected to remain high. In such a case, the short cracks would be able to propagate continuously within locally highly strained plastic zones. This effect appears to be the principal reason for the significant acceleration of short crack growth rates when the porosity becomes interconnected, as is shown in Fig. 4. Specifically, the interconnected porous materials will contain pores which are interconnected in a tubular fashion and furthermore these "tubes" will likely occur along grain boundaries. If this is the case and if a "tubular-shaped" pore is assumed to have a roughly constant diameter, then given the grain sizes typical in these materials, an estimate based on a plastic zone size which extends 1.5 times the average pore radius indicates that the grain adjacent to the pore will likely be fully encompassed by the plastic zone of the surrounding

pore. In the 6% interconnected material short cracks, surface observations have frequently indicated cracks linking with adjacent pores at high rates of growth. This is probably a result of the crack continually propagating in the highly strained plastic zone of the "tubular-shaped" pores and often within a single grain. This analysis also appears to be in agreement with those data in Fig. 4 which indicate that the maximum short crack growth rates in the interconnected and isolated porous materials are nearly the same, implying that these cracks probably propagated under similar maximum local strain amplitude conditions near pores.

The above observations in conjunction with the microstructural dissimilitude theory discussed previously can also be used as a basis for speculation regarding short crack behavior adjacent to a pore which is physically small (i.e. $\leq 100\mu\text{m}$ in diameter) but much larger than the grain size (i.e. $\sim 1\mu\text{m}$ diameter). Although this case is not experimentally verified in this study, our rationale indicates that, after propagating at a decelerating rate through a plastic zone of a physically small elliptically shaped pore, the short crack should approach the growth rate continuum predicted even for large cracks (see Fig. 7b). The large crack growth rate continuum is predicted for a physically small crack ($\sim 100\mu\text{m}$ in this example), because before the crack front extends through the plastic zone of the pore it will encounter several grains and therefore be microstructurally large. Thus, it is not surprising that the mechanically short crack growth profile predicted in Fig. 7b is similar to many of the profiles obtained from circular and elliptical notches scaling in size on the order of magnitude larger ($\sim 1\text{mm}$) in several other investigations.^(4-6,8)

Finally, the results obtained in this investigation indicate that for materials containing $\leq 6\%$ isolated porosity the pores should accelerate the short crack growth adjacent to the pore only in a region which scales with the pore size.

The vast majority of the short fatigue crack propagation life at these porosity levels occurs beyond the plastic zones of the pores where the cracks propagate at rates similar to those in a fully dense matrix (e.g. the sum of time that short cracks spend propagating within and out of the influence of the plastic zones is dominated by the periods of growth outside the plastic zones). Since the overall short crack growth rates appear to be dominated by the propagation behavior outside the realm of the pore-induced plastic zones, it appears that the fatigue life design criteria for short crack propagation behavior developed for fully dense materials should also be accurate when relatively small ($\leq 6\%$) volume fractions of isolated porosity is present. These results should apply not only to powder-processed materials, but also to cast or wrought materials which contain isolated porosity in which the pores are on the same order of magnitude as the grain size. It should be emphasized that these results do not imply that isolated porosity is not detrimental to low cycle fatigue life. In fact, even though the presence of isolated porosity does not appear to significantly influence the overall short fatigue crack growth rates, it is quite deleterious to low cycle fatigue life.⁽²⁴⁾ This latter behavior is the subject of current research.

Conclusions:

1. Isolated rounded porosity in the range of $\leq 6\%$ volume fraction of pores temporarily accelerates short fatigue crack growth as a result of locally high plastic strains within the pore-induced plastic zones. Outside the realm of these plastic zones (which scale with the pore size), short cracks propagate at rates which are similar to those which would be expected in a fully dense material (note that grain size effects on short crack growth persist in porous materials). For relatively low volume fractions of isolated porosity ($\leq 6\%$), most of the short crack propagation will occur primarily outside of the pore-induced

plastic zones, and the overall short crack growth rates will not be significantly influenced by the presence of pores.

2. At a level of 6% interconnected porosity and a total strain amplitude of 1.5%, short fatigue cracks propagate typically two to ten times faster than in the fully dense and isolated-porosity specimens. This appears to be a result of the short cracks propagating within the continuous plastic zone associated with the interconnected pores. These results imply that enhanced short crack propagation rates should also occur at higher levels of isolated porosity if the pores are sufficiently close to each other (≤ 2 pore diameters) such that the plastic zones overlap. For spherical isolated porosity, such spacings correspond to regions of (at least locally) high pore content, roughly 16% by volume.

3. Crack closure effects are negligible for short cracks in both the porous and fully dense titanium when undergoing fully reversible, large strain amplitude testing.

Acknowledgement

This research was supported by the Office of Naval Research through Contract NO. N00014-86-k-0381.

References:

1. Ritchie, R. O. and Lankford J., Eds, *Small Fatigue Cracks*, The Metallurgical Society, Inc., Warrendale, PA, 1986, 665 pp..
2. Miller, K. J. and de los Rios, E. R., Eds, *The Behaviour of Short Fatigue Cracks*, European Group on Fracture Pub. 1, Mechanical Engineering Publications Limited, London, 1986, 560 pp..
3. Oni, O. and Bathias, C., "Fatigue Crack Growth in Micro-notched Specimens of High Strength Steels," *Ibid*, pp. 295-307.

4. Foth, J., Marissen, R., Trautmann, K. H., and Nowack, H., **"Short Crack Phenomena in a High Strength Aluminum Alloy and Some Analytical Tools for Their Prediction,"** Ibid, pp. 353-368.
5. Lalor, P., Sehitoglu, H., and Mc Clung, R. C., **"Mechanics Aspects of Small Crack Growth from Notches - The Role of Crack Closure,"** Ibid, pp. 369-386.
6. Sehitoglu, H., **"Characterization of Crack Closure,"** *Fracture Mechanics: Sixteenth Symposium*, ASTM STP 868, M. F. Kanninen and A. T. Hopper, Eds, American Society for Testing Materials, Philadelphia, PA, 1985, pp. 361-380.
7. Heubaum, F. and Fine, M. E., **"Short Fatigue Crack Growth in a High Strength Low Alloy Steel,"** *Scripta Met.*, 18, 1984, pp. 1235-1240.
8. El Haddad, M. H., Smith, K. N., and Topper, T. H., **"A Strain Based Intensity Factor Solution for Short Fatigue Cracks Initiating from Notches,"** *Fracture Mechanics*, ASTM STP 677, C. W. Smith, Ed., American Society for Testing and Materials, Philadelphia, PA, 1979, pp. 274-289.
9. Gerard, D. A. **"The Influence of Porosity on Low Cycle Fatigue,"** Phd. Dissertation, Michigan Technological University, Houghton, MI, 1988.
10. Dowling, N. E., and Begley, J. A., **"Fatigue Crack Growth During Gross Plasticity and the J-Integral,"** *Mechanics of Crack Growth*, ASTM STP 590, American Society for Testing Materials, Philadelphia, PA, 1976, pp. 82-103.
11. Dowling, N. E., **"Geometry Effects and the J-Integral Approach to Elastic-Plastic Fatigue Crack Growth,"** *Cracks and Fracture*, ASTM STP 601, American Society for Testing Materials, Philadelphia, PA, 1976, pp. 19-32.
12. Dowling, N. E., **"Crack Growth During Low Cycle Fatigue of Smooth Axial Specimens,"** *Cyclic Stress-Strain and Plastic Deformation Aspects of Fatigue Crack Growth*, ASTM STP 637, American Society for Testing Materials, Philadelphia, PA, 1977, pp. 97-121.
13. Venkateswara Rao, K. T., Yu, W., and Ritchie, R. O., **"Fatigue Crack Propagation in Aluminum-Lithium Alloy 2090: Part II. Small Crack Behavior,"** *Metall. Trans. A*, 19A, 1988, pp. 563-569.

14. Douglas M. J. and Plumtree, A., "Application of Fracture Mechanics to Damage Accumulation in High Temperature Fatigue," *Fracture Mechanics*, ASTM STP 677, C. W. Smith, Ed., American Society for Testing Materials, Philadelphia, PA, 1979, pp. 68-84.
15. Starkey, M. S. and Skelton, R. P., "A Comparison of the Strain Intensity and Cyclic J Approaches to Crack Growth," *Fatigue of Engineering Materials and Structures*, 5, (4), 1982, pp. 329-341.
16. Starkey, M. S. and Irving, P. E. "Prediction of Fatigue Life of Smooth Specimen of SG Iron using a Fracture Mechanics Approach," *Low Cycle Fatigue and Life Prediction*, ASTM STP 770, American Society for Testing Materials, Philadelphia, PA, 1982, pp. 382-398.
17. Obrtlík, K. and Polák, J., "Fatigue Crack Growth of Surface Cracks in the Elastic-Plastic Region," *Fatigue Fract. Engng. Mater. Struct.*, 8, (1), 1985, pp. 23-31.
18. Klesnil, M., Polák, J., and Liskutín, P., "Short Crack Growth Close to the Fatigue Limit in Low Carbon Steel," *Scripta Met.*, 18, 1984, pp. 1231-1234.
19. Jolles, M., "Effects of Load Gradient on Applicability of a Fatigue Crack Growth Rate-Cyclic J Relation," *Fracture Mechanics: Sixteenth Symposium*, ASTM STP 868, M. F. Kanninen and A. T. Hopper, Eds, American Society for Testing Materials, Philadelphia, PA, 1985, pp. 381-391.
20. Wagner, L. and Lütjering, G., "Microstructural Influence on Propagation Behavior of Short Cracks in an ($\alpha + \beta$) Ti Alloy," *Z. Metallkde.*, 78, (5), 1987, pp. 369-375.
21. Robinson, J. L. and Beevers, C. J., "The Effects of Load Ratio, Interstitial Content, and Grain Size on the Low-Stress Fatigue Crack Propagation in α -Titanium," *Metal Science Journal*, 7, 1973, pp. 153-159.
22. Iyyer, N. S. and Dowling, N. E., "Opening and Closing of Cracks at High Cyclic Strains," *Small Fatigue Cracks*, R. O. Ritchie and J. Lankford, Eds., The Metallurgical Society, Inc., Warrendale, PA, 1986, pp. 213-223.
23. Chan, K. S. and Lankford, J., "The Role of Microstructural Dissimilitude in Fatigue and Fracture of Small Cracks," *Acta Metall.*, 36, (1), 1988, pp. 193-206.
24. Gerard, D. A. and Koss, D. A., to be published.

Table I

The thermo-mechanical processing history and the resulting grain and pore sizes for the wrought and powder-processed titanium. (The sintering and annealing treatments were performed in vacuum at $\sim 1 \times 10^{-5}$ torr.)

Wrought Ti (Fully Dense)	1.5% Porosity	6% Isolated Porosity	6% Interconnected Porosity
Machine LCF Specimen and polish ↓ Anneal 1 Hour @ 700°C ↓ 40μm Grain Size	Unsieved Powder ↓ Cold Isostatically Press to 380MPa ↓ Sinter 4 Hours @ 1300°C ↓ Swage: 18% Reduction in Area ↓ Sinter 4 Hours @ 1400°C ↓ Machine LCF Specimen and Polish ↓ Anneal 1 Hour @ 700°C ↓ 100μm Grain Size And ~30μm Average Pore Diameter	Sieved Powder (-106μm to +38μm) ↓ Cold Isostatically Press to 380MPa ↓ Sinter 4 Hours @ 1300°C ↓ Machine LCF Specimen and Polish ↓ Anneal 1 Hour @ 700°C ↓ 40μm Grain Size And ~30μm Average Pore Diameter	Sieved Powder (-177μm to +125μm) ↓ Cold Isostatically Press to 380MPa ↓ Sinter 4 Hours @ 1400°C ↓ Machine LCF Specimen and Polish ↓ Anneal 1 Hour @ 700°C ↓ 80μm Grain Size And ~55μm Average Pore Diameter

Table II

The chemical analyses (wt. %) for the wrought and the powder processed titanium.

Element	Wrought Ti	Ti Powder	Processed Ti Powder
O	.130	.099 - .135	.131 - .146
H	<.005	.0005 - .0019	.0001-.0006
C	.010	.0030 - .0080	.007
Cl	---	.015 - .018	.008
Fe	.040	.0050 - .0074	.006
N	.010	.0032 - .0080	.005

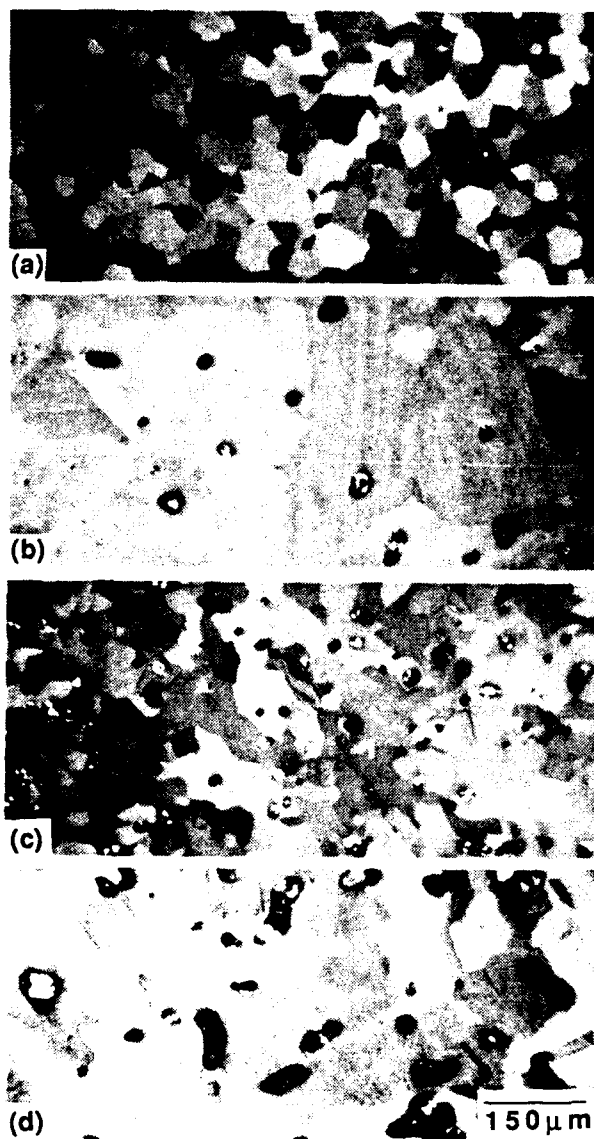


Figure 1. Polarized light micrographs of titanium containing (a) 0% porosity, (b) 1.5% isolated porosity, (c) 6% isolated porosity and (d) 6% interconnected porosity. The bright reflections are from epoxy used to preserve the original pore shape during polishing. All the micrographs have the same magnification.

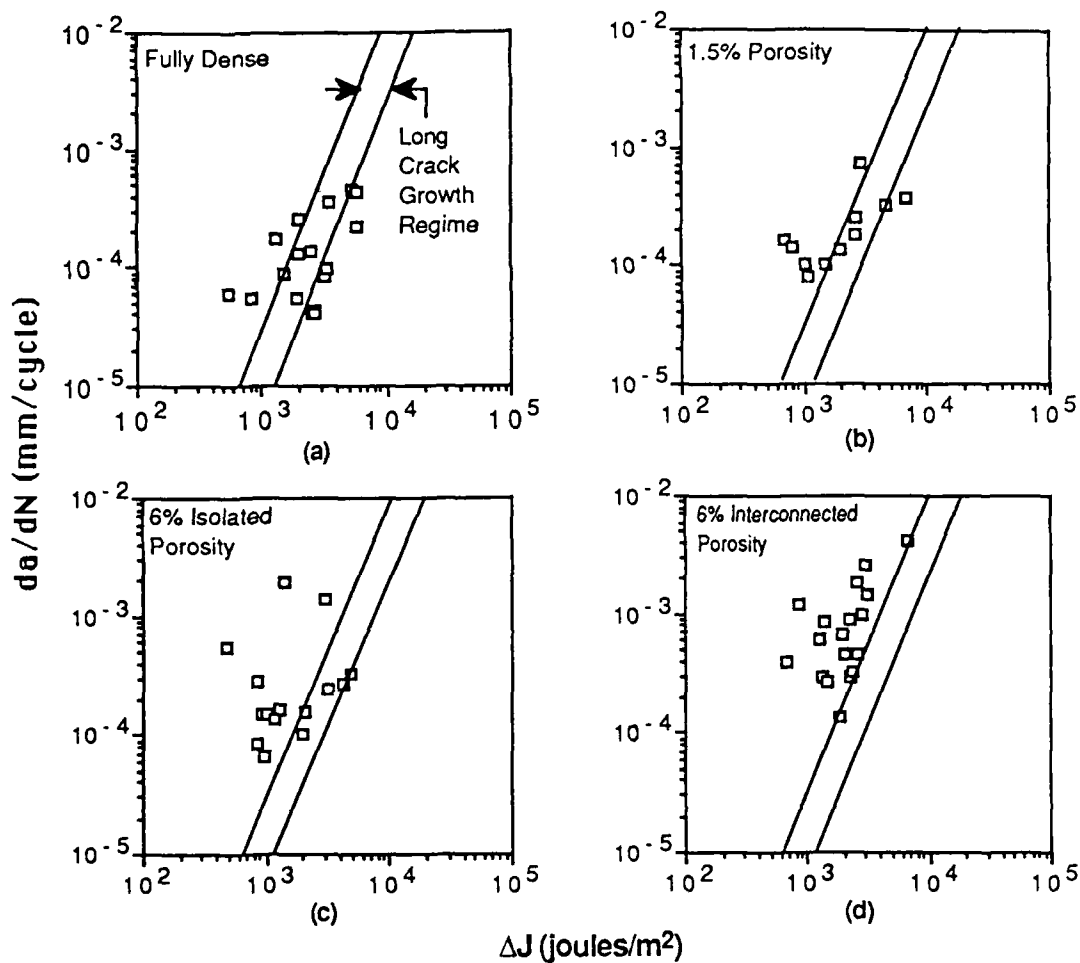


Figure 2. The dependence of short crack growth rates on ΔJ as measured during 1.5% total strain amplitude testing for titanium which has (a) 0% porosity, (b) 1.5% isolated porosity, (c) 6% isolated porosity, and (d) 6% interconnected porosity. The two solid lines in each plot indicate an extrapolated range of the long crack growth data obtained by Robinson and Beevers⁽²¹⁾ for fully dense titanium of similar purity to that used in this investigation.

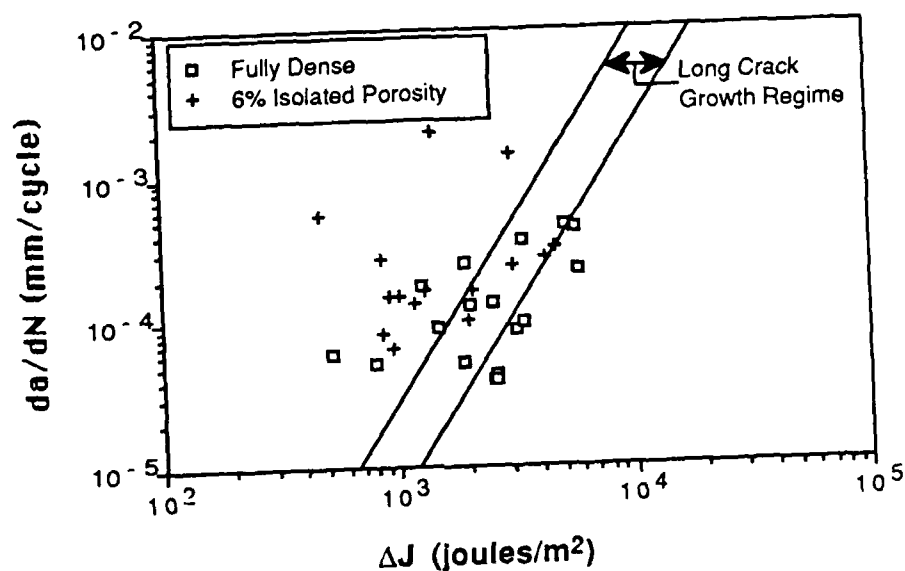


Figure 3. The dependence of the short crack propagation rates on ΔJ as determined for fully dense and 6% isolated porosity materials examined at a total strain amplitude of 1.5%. The two solid lines indicate the extrapolation of data from the large crack growth regime as measured by Robinson and Beevers⁽²¹⁾ for fully dense titanium of similar purity to that used in this examination.

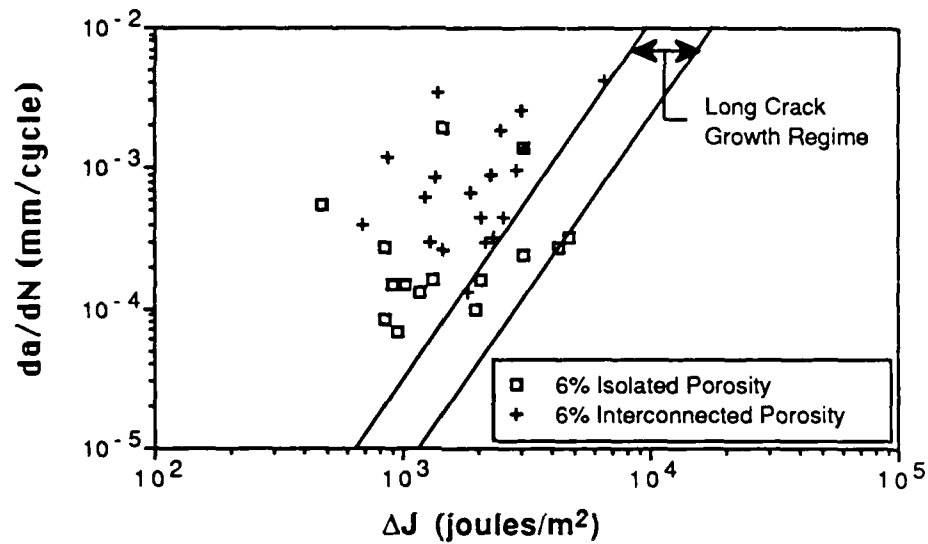


Figure 4. Comparing the short crack propagation rates for the 6% porous titanium containing isolated and interconnected porosity and tested at 1.5% total strain amplitude. The two solid lines encompass data extrapolated from the large crack growth regime by Robinson and Beevers⁽²¹⁾ for fully dense titanium of similar purity to that used in this investigation.

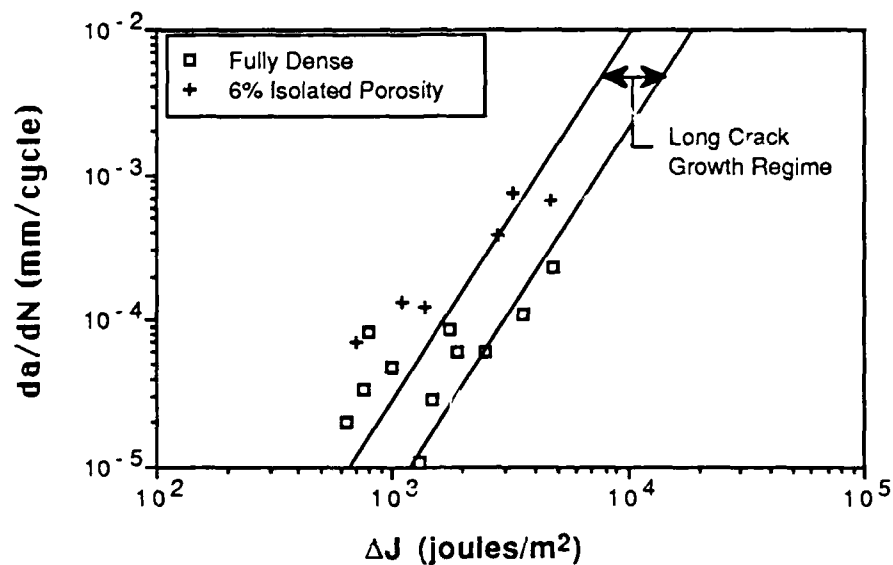


Figure 5. The dependence of the short crack growth rates on ΔJ for the fully dense and the 6% isolated porosity titanium tested at 0.75% total strain amplitude. The two solid lines are extrapolations of the linear elastic long crack growth regime data as measured by Robinson and Beevers⁽²¹⁾ for fully dense titanium of similar purity to that used in this study.

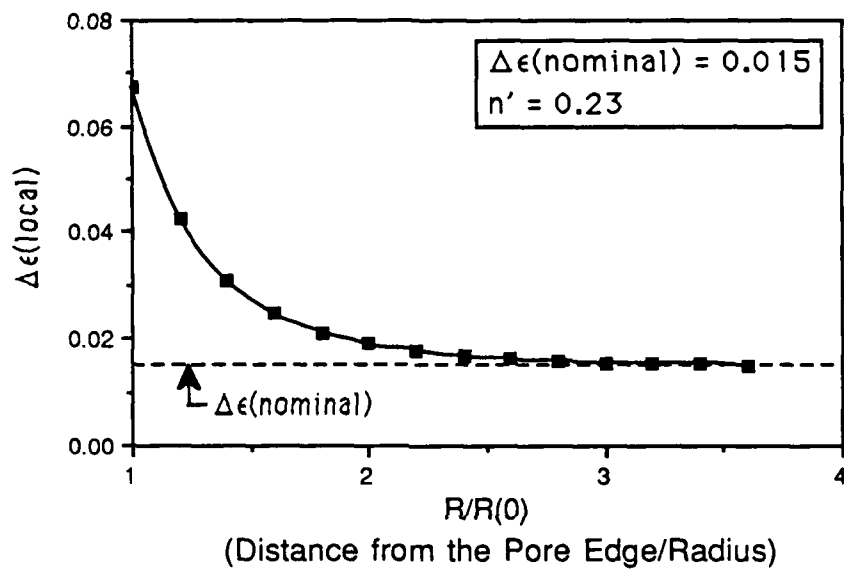


Figure 6. A theoretical profile of a local strain amplitude distribution adjacent to an elliptical pore in a plastically deforming matrix. The profile has been estimated at the peak tensile load of a cycle on the plane of maximum strain concentration over a normalized distance $R/R(0)$. The elliptical pore has an aspect ratio of ~ 1.3 with the minor diameter being normal to the fatigue axis.

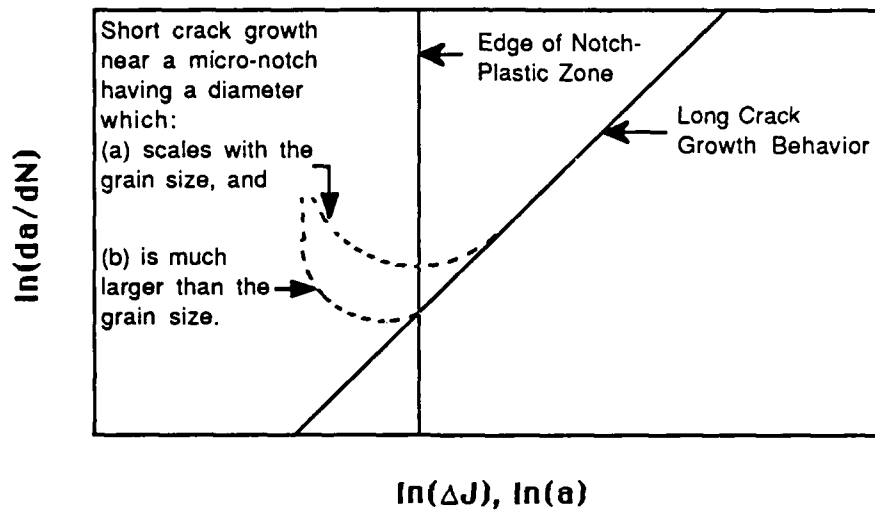


Figure 7. Schematic profiles of short crack growth behaviors in the presence of a microscopic elliptical notch which (a) scales with the grain size, and (b) is much larger than the grain size. The dotted vertical line indicates the boundary between the plastic zone adjacent to a micro-notch and the plastically deforming matrix; recall that $\Delta J \propto a$.